

Ground-Based GPS for Validation of Climate Models: The Impact of Satellite Antenna Phase Center Variations

Per Jarlemark, Ragne Emardson, Jan Johansson, and Gunnar Elgered

Abstract—The amount of water vapor in the atmosphere is an important indicator for climate change. Using the Global Positioning System (GPS), it is possible to estimate the integrated water vapor (IWV) above the ground-based GPS receiver. In order to optimally determine the IWV, a correct model of the received signal phase is essential. We have studied the effect of the satellite antenna phase center variations (PCVs) on the IWV estimates by simulating the effect and by studying the estimates of the IWV based on the observed GPS signals. During a period of five years, from 2003 to 2008, a new satellite type was introduced, and it steadily grew in numbers. The antenna PCVs for these satellites deviate from the earlier satellite types and contribute to excess IWV estimates. We find that ignoring satellite antenna phase variations for this time period can lead to an additional IWV trend of about $0.15 \text{ kg/m}^2/\text{year}$ for regular GPS processing.

Index Terms—Antennas, error analysis, Global Positioning System (GPS), meteorology.

I. INTRODUCTION

ATMOSPHERIC water vapor feedback is thought to amplify the global climate response to increased concentrations of greenhouse gases [1]. Hence, for modeling climate change, one of the most important challenges is to properly account for water vapor in the climate warming [2]. The Global Positioning System (GPS) is a useful tool for measuring the atmospheric water vapor. In state-of-the-art GPS data processing, the observed signal phase at the receiver is used to estimate the integrated water vapor (IWV) above the receiving antenna. Many of such studies have been performed using networks of permanently installed GPS receivers [3]–[8]. A correct model of the received signal phase is essential in optimally determining the IWV from GPS. Unmodeled effects may otherwise propagate into the estimated IWV and may thus be misinterpreted as an additional water vapor. Fig. 1 shows an example of the estimated IWV from GPS at the permanent International GPS Service (IGS) site Onsala on the Swedish west

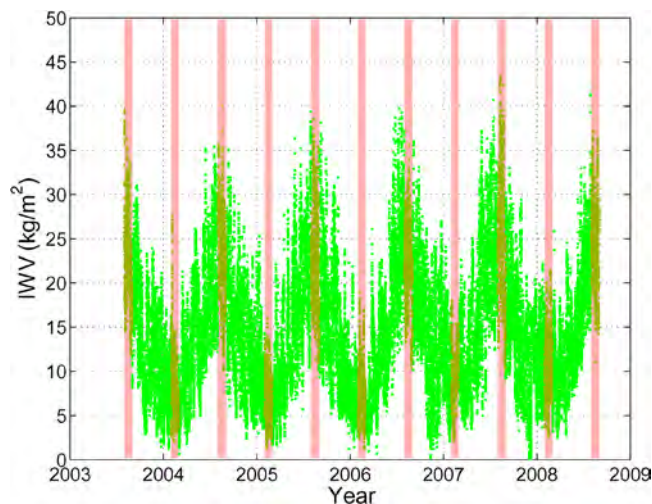


Fig. 1. Example of the estimated IWV from GPS at the Onsala site on the Swedish west coast. The results are obtained using GIPSY [9]. The shaded areas in the figure illustrate the months (August and February) used in this paper.

coast. The results are obtained using the GPS-Inferred Positioning System (GIPSY) software [9] and the Emardson–Derks simplified physical model [10] for conversion to IWV. The agreement of the results with IWV measurements from ground-based microwave radiometry is typically $1\text{--}2 \text{ kg/m}^2$ in terms of daily root-mean-square differences [4]. Eleven periods with a duration of one month are shown in Fig. 1. These periods are used in order to investigate the effects of the antenna phase variations.

In the next section, we illustrate the antenna phase variations. The experimental setup and the parameters estimated in the GPS processing are described in Section III, followed by the results in Section IV. Sections V–VII contain the simulated effects, where we have studied the dependence on satellite observation distribution and station latitude, respectively. In Section VIII, we discuss the results and explain why the IWV estimates are affected by unmodeled signal phase variations and the relation between the IWV and vertical position coordinate estimates. Section IX ends this paper with the conclusion.

II. BACKGROUND

In GPS processing, all measurements are described as originating from an electrical phase center of the satellite antenna. However, the force models used for the orbit modeling apply for

Manuscript received May 20, 2009; revised October 23, 2009 and February 16, 2010. This work was supported by VINNOVA (Swedish Governmental Agency for Innovation Systems) through project P29459-1 “Long Term Water Vapour Measurements Using GPS for Improvement of Climate Modelling.”

P. Jarlemark, R. Emardson, and J. Johansson are with the SP Technical Research Institute of Sweden, 501 15 Borås, Sweden (e-mail: per.jarlemark@sp.se; ragne.emardson@sp.se).

G. Elgered is with the Department of Radio and Space Science, Onsala Space Observatory, Chalmers University of Technology, 43 992 Onsala, Sweden

Color versions of one or more of the figures in this paper are available online at <http://ieeexplore.ieee.org>.

Digital Object Identifier 10.1109/TGRS.2010.2049114

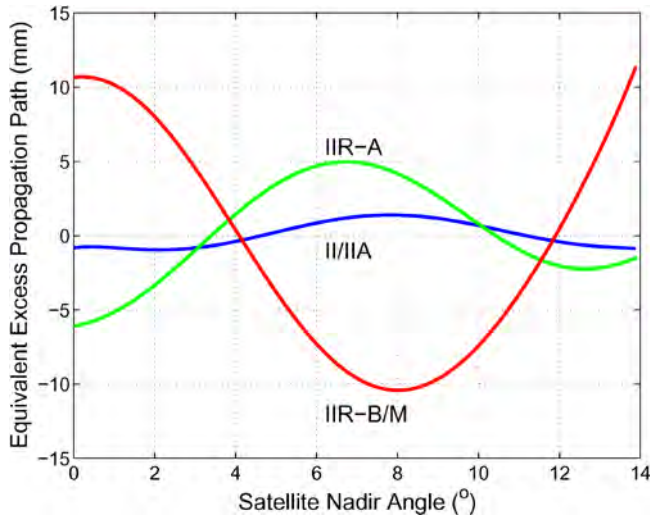


Fig. 2. Antenna PCVs for the three satellite types: (blue) II/IIA, (green) IIR-A, and (red) IIR-B/M.

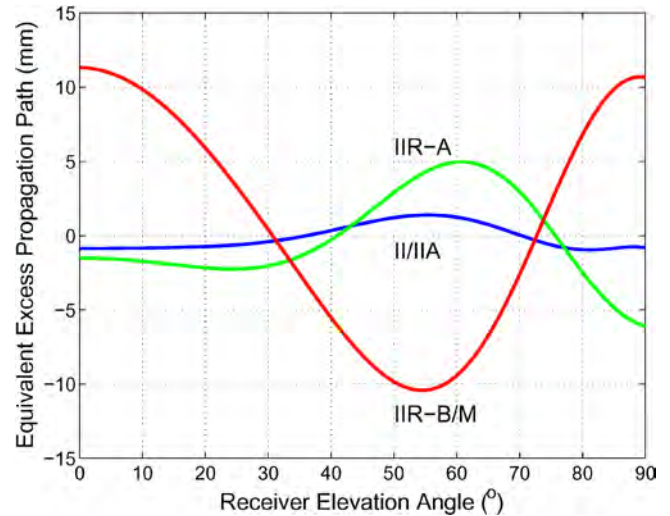


Fig. 3. Antenna PCVs for the three satellite types: (blue) II/IIA, (green) IIR-A, and (red) IIR-B/M.

63 the center of mass. Hence, the precise satellite coordinates and
 64 clock products used in much state-of-the-art processing refer
 65 to the center of mass of the satellites [11]. Difficulties to find
 66 the distance between the phase and mass centers lead to an
 67 inconsistency of the GPS observations. For each GPS satellite,
 68 such a distance between the antenna phase center and the center
 69 of mass does exist. However, studies [12] have shown that this
 70 distance consists of the following: 1) mean value, i.e., a phase
 71 center offset (PCO), and 2) variations as a function of the nadir
 72 angle, i.e., a phase center variation (PCV). Schmid *et al.* [12]
 73 model PCVs for three different satellite types as a function of
 74 the nadir angle based on several years of GPS observations.
 75 Fig. 2 shows the PCVs for the three satellite types presently
 76 in use, i.e., II/IIA, IIR-A, and IIR-B/M. Unmodeled phase
 77 variations at the satellite antenna are observed as an elevation-
 78 dependent additional phase delay at the receiving antenna.

79 The pattern can be transformed to an elevation-dependent
 80 additional phase delay, as seen by the receiver on the ground.
 81 Fig. 3 shows the phase delay as a function of the elevation an-
 82 gle. Most elevation-angle-dependent error sources have a large
 83 influence on both the vertical coordinate of the position estimate
 84 and the estimate of the signal delay due to the atmosphere,
 85 which in turn maps to the IWV values.

86 As shown in Fig. 3, the amplitude of the PCV is larger for
 87 the satellites of type IIR-B/M. The number of satellites of type
 88 IIR-B/M has steadily increased during the experiment period
 89 from 0 to 10. Fig. 4 shows the number of each satellite type
 90 during this period. The increase of the type IIR-B/M satellites
 91 has been at the expense of the type II/IIA satellites.

92 In much of the state-of-the-art GPS processing prior to
 93 November 6, 2006, the vertical component of the PCO, i.e.,
 94 the direction pointing toward the center of earth, was assumed
 95 to be 1.023 m for the satellites of type II/IIA and zero for the
 96 other satellite types. In processing, since that date, the PCOs
 97 shown in Fig. 5 have been applied separately for each satellite
 98 for the entire life of the satellite. Fig. 5 shows the recommended
 99 PCO for each satellite in use during our study period [13].
 100 A constant value of 1.023 m, which was used previously, is

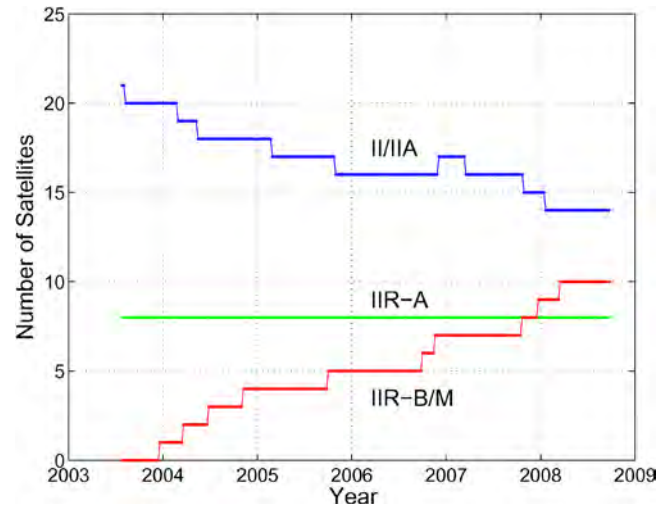


Fig. 4. Number of satellites of types (blue) II/IIA, (green) IIR-A, and (red) IIR-B/M from 2003 to 2008.

101 already removed from the satellites of type II/IIA. Hence, what
 102 is shown is the additional knowledge after the determination of
 103 separate phase offsets.

104 In addition to the modeling of the satellite antennas, a similar
 105 work was performed for the ground receiver antennas. A set
 106 of PCOs (rPCO) and PCVs (rPCV) was derived for different
 107 receiver antenna types [13].

108 We have studied the effect of satellite antenna phase vari-
 109 ations mainly on the IWV estimates and the implication for
 110 climate interpretations. That is, we have primarily focused on
 111 the effects of the PCO and PCV models presented earlier. We
 112 have chosen sites where no changes have been made to the
 113 receiving antennas during our period of study, and thus, the
 114 rPCO and rPCV have an insignificant effect on the estimated
 115 IWV trends. This paper has been performed both by simulating
 116 the effects and by studying the estimates based on the observed
 117 data. We have used observations from three permanent IGS
 118 sites [14] at three different latitudes, namely, Onsala, Sweden, 118

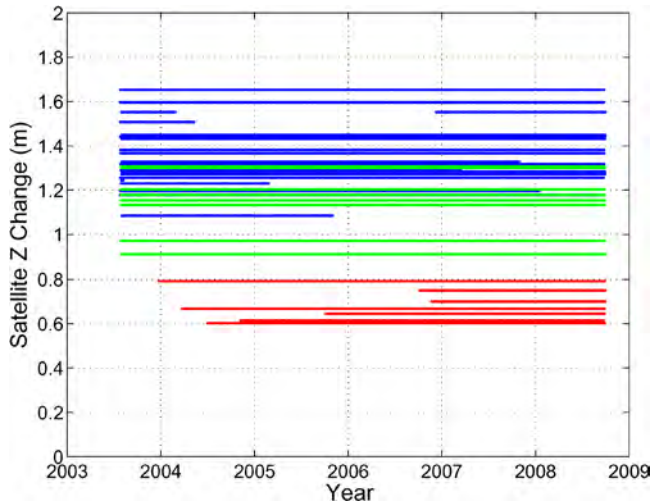


Fig. 5. Change in the applied satellite antenna vertical PCO for each satellite in use from 2003 to 2008. The colors indicate the type of satellite with the coding (blue) I/I/A, (green) IIR-A, and (red) IIR-B/M.

119 at 57° N; Matera, Italy, at 41° N; and Kourou, French Guiana,
120 at 5° N.

121

III. EXPERIMENTAL SETUP

122 We have studied the effect of the satellite PCOs and PCVs
123 on the IWV estimates both by studying the estimates of the
124 IWV using observed GPS signals and by simulating the effects.
125 In both cases, the data have been processed using a Kalman
126 filter technique (e.g., see [15]), which is a minimum variance
127 estimation algorithm in the special case where the system is
128 a linear stochastic dynamical system. The main model of the
129 filter is the assumed linear relationship between measurements
130 z and the variables x that we want to estimate. This relationship
131 is described by the observation matrix H containing the partial
132 derivatives

$$z = Hx + v \quad (1)$$

133 where v is the measurement noise.

134 The observed GPS signals were processed with the GIPSY
135 v4.04 software using the precise point positioning (PPP)
136 method [9] based on the satellite orbits provided by the Jet
137 Propulsion Laboratory. Hence, we solve, in the processing, for
138 the 3-D station coordinates, the atmospheric zenith total delay,
139 and the receiver clock offset. The processing of the data with
140 the correction models applied was performed by correcting the
141 effects directly in the Receiver Independent Exchange Format
142 observation files prior to the processing (GIPSY software v5.0
143 includes an option to correct for such effects.).

144 We performed simulations based on the PCO and PCV
145 models. The simulations were carried out in order to display
146 the difference in the resulting IWV with and without the cor-
147 rection models. In this paper, we consider this difference in the
148 resulting IWV as the error in the IWV results. The simulations
149 were performed in MATLAB using an in-house simulation
150 software package, with the modeling and processing strategy
151 imitating the PPP method [9]. All process parameters were
152 identical for all simulations and identical to those in the GIPSY
153 processing. In our application, the formulation of the Kalman

filter equations is almost perfectly linear when estimating a set
of variables x from (1), i.e.,

$$\hat{x}(z + \delta z) = \hat{x}(z) + \hat{x}(\delta z) \quad (2)$$

for small errors δz . Hence, these errors can be treated sepa-
rately to derive their effects $\hat{x}(\delta z)$ on the sought variables. We
constructed simulated measurement errors based on the models.
These errors were used as input to the simulation software, as
 δz in the Kalman filter formulation. No other errors were fed
into the simulation software. This strategy provides the error in
the zenith wet delay, given the simulated measurement errors
and, thus, the corresponding error in the IWV.

Normally, when determining the IWV from the total at-
mospheric delay estimates, we subtract a hydrostatic part [16]
from the total delay based on independent pressure measure-
ments and thus obtain the delay in the atmosphere mainly due
to water vapor, i.e., the wet delay. The wet delay can be used
to estimate the IWV based on temperature-dependent scaling
factors (e.g., see [10]). In this paper, however, we evaluate the
difference in the IWV estimates from the solutions by changing
only the PCV and PCO models. Hence, the hydrostatic delay is
identical in the solutions and is therefore cancelled when calcu-
lating the difference. For the same reason, in the following, we
use a simplified conversion factor of 6.3-mm atmospheric delay
per kg/m^2 IWV [10].

For both observed and simulated data, we studied a period
from mid 2003 to mid 2008. We have chosen two months
(February and August) every year for the processing. During
these months, we estimated the IWV every 5 min. We studied
the effects of using only observations above a specific elevation
angle, i.e., an elevation cutoff angle. The cutoff angles that we
used were 5° , 10° , 15° , and 20° . Today, the cutoff angles 10°
and 15° are the most commonly used, and hence, the focus was
on those results.

IV. EFFECTS OF ANTENNA MISMODELING

As described in the previous section, we can process the
GPS observations both with and without applying the antenna
phase center corrections. Fig. 6 shows the difference in the
estimated IWV between these two solutions for the Onsala site.
The blue triangles illustrate the mean values for each month.
The red line in the figure is the least square fit to the estimated
IWV differences. The slope of this line is $0.071 \text{ kg/m}^2/\text{year}$,
with a 1σ uncertainty of $0.005 \text{ kg/m}^2/\text{year}$. Hence, ignoring
the antenna phase variations when processing the GPS data
from this time period can lead to a misinterpretation of an
additional IWV trend of about $0.07 \text{ kg/m}^2/\text{year}$ for this type
of GPS processing, assuming that the models are correct. The
uncertainty is based on the use of a straight line to fit the
data points, given a χ^2 per degree of freedom that is equal to
one. The uncertainty says nothing about the validity of such a
straight line model. A straight line is, however, a reasonable
model when studying climate variations.

In the figure, in addition to the PCO and PCV effects, the
rPCO and rPCV effects are also included for the completeness

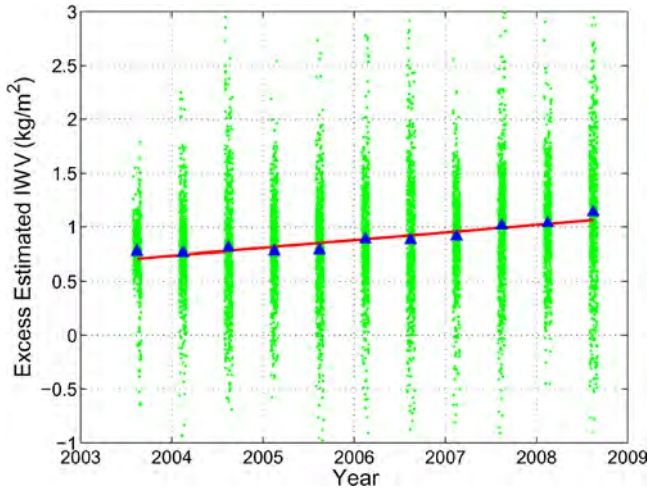


Fig. 6. Error in the estimated IWV when omitting the PCO, PCV, rPCO, and rPCV corrections. The figure shows the estimated IWV without corrections minus the estimated IWV with corrections. The observed data are acquired at Onsala and are processed with an elevation cutoff angle of 10° .

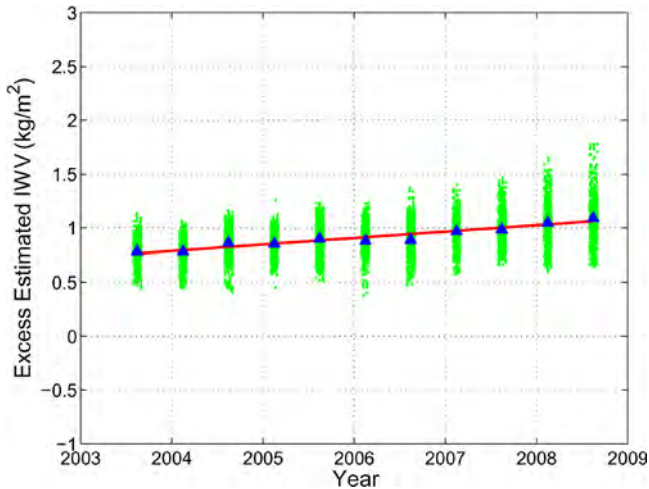


Fig. 7. Simulated error in IWV when omitting the PCO, PCV, rPCO, and rPCV corrections. The figure shows the IWV without corrections minus the IWV with corrections. The data are simulated for the Onsala site and are processed with an elevation cutoff angle of 10° .

206 of the GPS solution. The contribution from the latter two is, 207 however, only a constant offset value.

208 Fig. 7 shows the results from the simulations. Also in this 209 figure, the rPCO and rPCV effects are included in order to 210 imitate the solution based on the observed data. The results of 211 the simulations are similar (both concerning the slope and the 212 offset) to the results based on the observations. The slope of the 213 straight line here is $0.059 \text{ kg/m}^2/\text{year}$, with a 1σ uncertainty of 214 $0.001 \text{ kg/m}^2/\text{year}$. This uncertainty value is a representative of 215 the simulated results in this paper. Note also the variations in the 216 simulated results within each monthly batch. These originate 217 from the small differences in the satellite constellation from day 218 to day.

219 V. CONTRIBUTIONS FROM DIFFERENT COMPONENTS

220 As seen in the previous section, the use of the antenna phase 221 center models in the GPS processing affects the estimated IWV. 222 By simulating these variations, we can separate the different

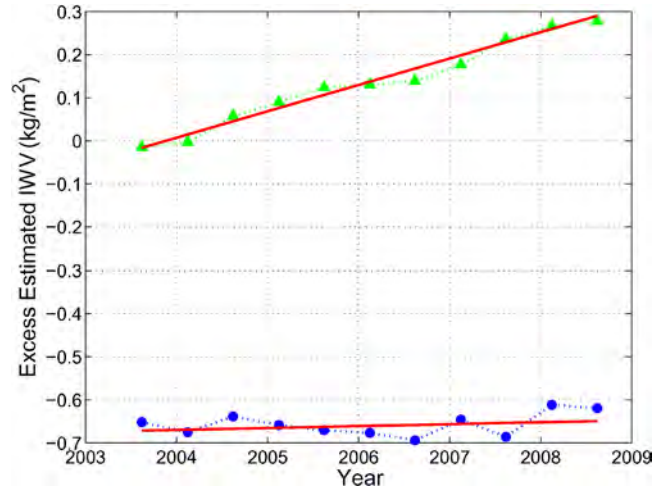


Fig. 8. Simulated error in IWV when omitting the (blue circles) PCO and (green triangles) PCV corrections. The figure shows the IWV without corrections minus the IWV with corrections. The red straight lines are the least square fits to the data points.

223 effects and their respective influence on the results. Now, we 224 study the influence of the PCV and PCO models separately on 225 the estimated IWV for the Onsala site using a cutoff angle of 226 10° . The results are produced similarly to the results in the 227 previous section. For clarity, we show the results as monthly 228 average values, i.e., two values per year. Fig. 8 shows the 229 simulated effects on the estimated IWV by applying the PCO 230 and PCV corrections separately. Note that the rPCO and rPCV 231 corrections are not taken into account. Hence, results are not 232 directly comparable to those in Fig. 7. The effect of the PCO is 233 a relatively insignificant trend in the estimates, while applying 234 the PCV results in an increase of approximately 0.3 kg/m^2 over 235 the five-year period. Hence, processing the GPS observations 236 during this period without applying the PCV models produces 237 results that can be misinterpreted as an existing IWV trend of 238 $0.06 \text{ kg/m}^2/\text{year}$.

239 Fig. 9 shows the effects on the estimated vertical position 240 component of applying the PCO and PCV corrections. For the 241 vertical coordinate estimate, the effect of applying the PCO, 242 approximately 5 mm over the five-year period, is dominating 243 over the effect of applying the PCV. This result is the opposite 244 of what we found for the IWV estimate. Hence, processing the 245 GPS observations during this period without applying the PCO 246 models produces results that can be misinterpreted as a vertical 247 change of -1 mm/year .

248 It is important to remember that, in our simulations, we have 249 not included the effects on orbit and satellite clock estimation 250 and their secondary effect on the estimates, which could have 251 an effect on parts of the results. However, we do not believe 252 that the inclusion of this effect has any significant impact on the 253 IWV results of the PCV simulations due to the relatively rapid 254 spatial variations, as seen from a tracking network, of the PCV 255 compared to those of the satellite orbits and clock parameters.

256 VI. ELEVATION DEPENDENCE

257 The previous results were produced using an elevation 258 cutoff angle of 10° . We know from several studies of 259

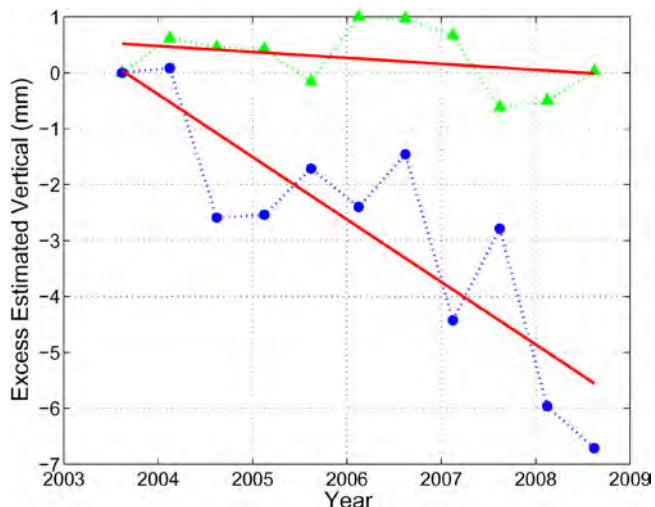


Fig. 9. Simulated variation in vertical positions when omitting the (blue circles) PCO and (green triangles) PCV corrections. The figure shows the position without corrections minus the position with corrections. The results are adjusted so that the results for the first month are zero. The red straight lines are the least square fits to the data points.

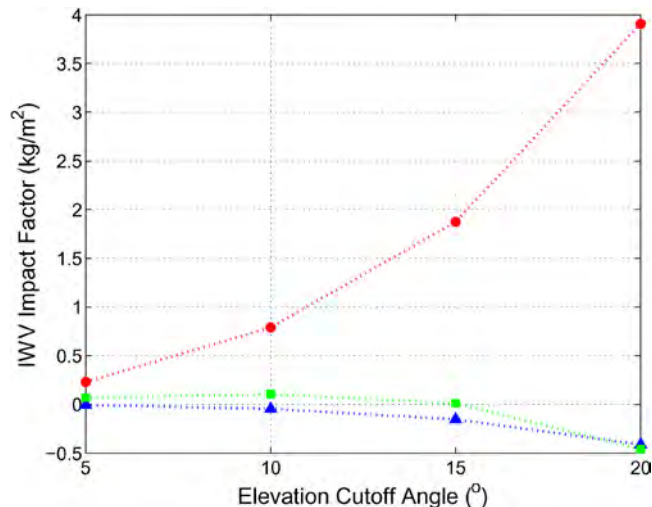


Fig. 10. Simulated contribution to the IWV estimates from the different satellite types, namely, (blue triangles) II/IIA, (green squares) IIR-A, and (red circles) IIR-B/M, for different cutoff angles.

259 elevation-dependent error sources that the results may vary
 260 significantly if the elevation cutoff angle is changed. Thus, we
 261 studied the impact of the chosen cutoff angle on the IWV by
 262 simulations. We include only the PCV when investigating the
 263 elevation dependence due to the minor effect that the PCO has
 264 on the estimate of a trend in the IWV. In order to illustrate
 265 the different contributions at different elevation cutoff angles,
 266 we study each satellite type separately. Fig. 10 shows the
 267 contribution on the IWV estimates from the different satellite
 268 types for elevation cutoff angles ranging from 5° to 20°. The
 269 results in the figure are produced using the constellation of
 270 February 15, 2006, at the Onsala site. However, the errors in
 271 the IWV estimates are based on a hypothetical scenario that all
 272 satellites are of only one type. By combining the information of
 273 Fig. 10 with the relative amount of the different satellite type, it
 274 is possible to obtain a rule of thumb for the impact on the IWV
 275 estimate at different times.

276 Fig. 11 shows the relative number of the different satellite
 277 types. By multiplying the relative occurrence of the satellite
 278 types with their corresponding impact factor, the excess
 279 IWV at a certain time and the elevation cutoff angle can be
 280 approximated.

281 VII. LATITUDE DEPENDENCE

282 The observation angles to the GPS satellites will differ for
 283 sites at different latitudes. As the elevation cutoff angle has a
 284 clear effect on the impact of the unmodeled PCV, we can expect
 285 that the distribution of the observations and, thus, the latitude of
 286 the GPS receiver also have an impact. Fig. 12 shows the satellite
 287 coverage for the Onsala, Matera, and Kourou sites together
 288 with the number of binned observations for elevation angles
 289 between 0° and 90°. The number of high-elevation observations
 290 is relatively similar for the three sites. One could believe that
 291 the number of high-elevation observations should be lower for
 292 the most northern sites due to the coverage, as seen in a polar
 293 plot. This is, however, not the case due to the slower passage at

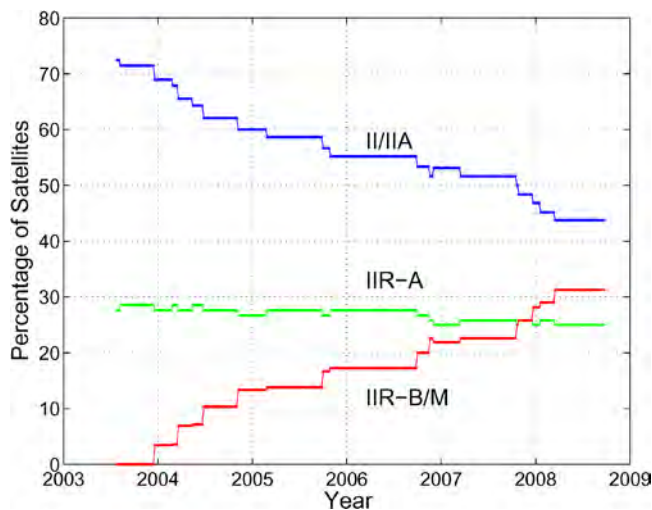


Fig. 11. Relative number of satellites of types (blue) II/IIA, (green) IIR-A, and (red) IIR-B/M as percentage of the total number of satellites from 2003 to 2008.

high elevations of the satellites over these sites. For the Kourou 294
 site, the number of observations at elevation angles between 15° 295
 and 30° is significantly higher than for the other sites, while 296
 the number of observations above an elevation of 60° is lower. 297
 These differences in the distribution of the observations have 298
 an impact on how the unmodeled elevation-dependent effects 299
 propagate into the IWV estimates. 300

As the choices of the elevation cutoff angle and the latitude 301
 of the GPS location have an impact on the estimated IWV, we 302
 can, by analogy with Fig. 8, study the trends in the estimated 303
 IWV for the three sites that we have chosen for this paper and 304
 for the most commonly used elevation cutoff angles. Table I 305
 shows such estimated slopes for the three sites in the study for 306
 10° and 15° cutoff angles. As indicated previously, the effect on 307
 the IWV trend is larger for the solutions processed with higher 308
 elevation cutoff angles. This is the case for all three sites. We 309
 also notice that the effect is much less significant for the Kourou 310
 site than for the other two, which have very similar results. 311

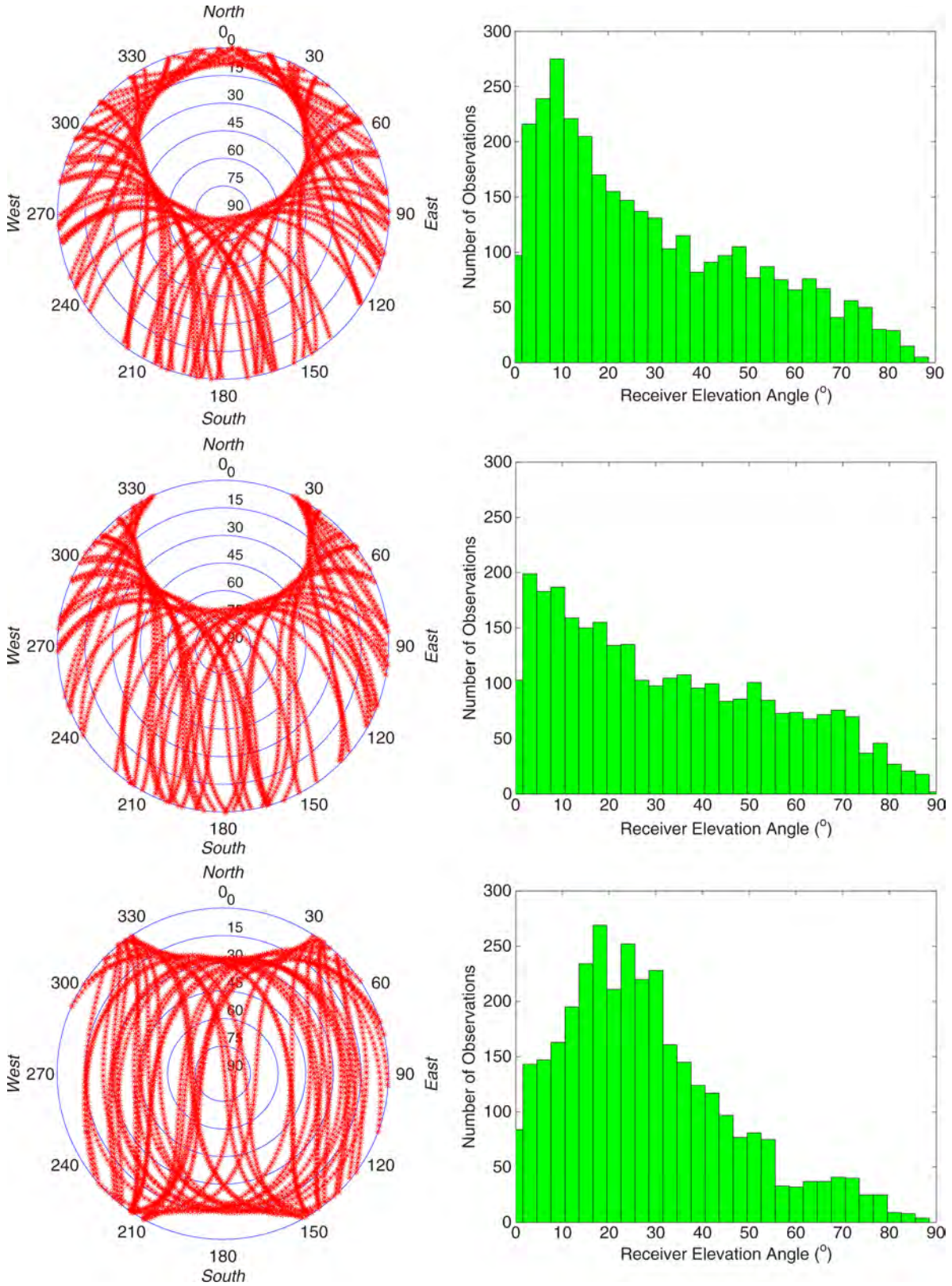


Fig. 12. Satellite coverage for the (top) Onsala, (middle) Matera, and (bottom) Kourou sites. The observations are acquired every 5 min during one day.

312

VIII. DISCUSSION

313 A general problem with using least square techniques such
 314 as Kalman filtering is that unmodeled effects in the observa-
 315 tions propagate into the estimates of the sought parameters.

The better this unmodeled effect happens to match the partial
 316 derivatives, modeling the relation between the observations
 317 and the parameters, the greater is the influence on the sought
 318 parameters. In GPS processing, the elevation-dependent effects
 319

TABLE I
SIMULATED EFFECT ON THE IWV ESTIMATES IF THE PCVs ARE NOT TAKEN INTO ACCOUNT. THE SLOPES ARE BASED ON AN OBSERVATIONAL PERIOD FROM MID 2003 TO MID 2008. THE 1σ UNCERTAINTIES FOR THE SLOPE ESTIMATES ARE 0.001 AND 0.002 kg/m²/year FOR THE CUTOFF ANGLES 10° AND 15°, RESPECTIVELY

Site	Latitude °N	IWV Slope (kg/m ² /year) Cutoff Angle	
		10°	15°
Onsala	57	0.06	0.14
Matera	41	0.08	0.16
Kourou	5	0.03	0.08

320 tend to propagate into a combination of a vertical movement of
321 the site, an atmospheric delay change, and a change in the site's
322 clock offset.

323 A specific elevation-dependent unmodeled error can thus
324 affect only the vertical estimates, while another can affect the
325 estimates of the atmospheric delay change only. In most cases,
326 both the vertical and atmosphere delay estimates are influenced,
327 but as shown in this paper, the elevation-dependent errors
328 exist, which, to a large extent, only have an impact on one of
329 the estimated parameters.

330 As shown in Fig. 3, the PCVs are elevation-dependent
331 effects. Not modeling these PCVs results in errors in the
332 estimated atmospheric zenith total delay and, thus, also in
333 the IWV estimates. The PCV can relatively well be described
334 by the partial derivatives at higher elevation angles. However,
335 the partial derivative representing the delay due to the neutral
336 atmosphere is large below 30°, and it grows rapidly with lower
337 elevation angles. Its elevation dependence can be approximated
338 by the function 1/sin(elevation). The PCV of satellite type
339 IIR-B/M, in contrast to the earlier types, has a pronounced
340 signature at lower elevation angles, e.g., below 30°. Although
341 strong, this signature is relatively small compared to the partial
342 derivative representing the atmospheric delay. That is, process-
343 ing without the PCV model, observations at low elevation
344 angles will contradict an interpretation of a strong excess IWV
345 component, also for observations of satellite type IIR-B/M.

346 As a consequence, low-elevation-angle observations are
347 beneficial for the GPS processing that is ignoring the PCV
348 corrections. Even when taking into account the PCV, low-
349 elevation-angle observations may be useful (e.g., [17]), for
350 example, by reducing the effect of other elevation-dependent
351 error sources. Also, the latitude dependence seen in Section VII
352 can be explained by the influence of low-elevation observations.
353 At Kourou, with its relatively high number of observations
354 below 30°, a significantly smaller sensitivity to the satellite type
355 IIR-B/M introduction is seen.

356 Down weighting of low-elevation observations when
357 processing GPS data is a common practice and is beneficial for
358 different reasons. However, performing down weighting while
359 omitting the satellite antenna PCV in the processing reduces
360 the positive effect of the low-elevation observations. Hence, this
361 can, in specific cases, lead to larger errors.

362 IX. CONCLUSION

363 Processing of GPS data without the inclusion of correct
364 antenna models leads to an error in the IWV estimate. In

particular, omitting the satellite antenna PCV causes an appar- 365
ent trend in the IWV. For example, it can lead to an additional 366
IWV trend of up to 0.15 kg/m²/year for regular GPS processing 367
for the time period 2003–2008. Although we have selected an 368
inauspicious period, given the changes of the satellite types, 369
this can be compared to linear trends estimated from Swedish 370
and Finnish GPS data (without using corrections for antenna 371
PCVs) that are acquired over a ten-year period, which range 372
from −0.05 to 0.1 kg/m²/year[7]. 373

The apparent trend depends on the growing number of satel- 374
lites of type IIR-B/M. The size of the apparent trend varies with 375
the latitude of the observing site, the chosen elevation cutoff 376
angle, and the weighting of the observations. In general, obser- 377
vations at low elevation angles with relatively high weighting 378
reduce the effect. 379

Normally, by keeping the configuration fixed in GPS process- 380
ing, we do not expect false trends in the time series of the 381
estimates. Changes in, for example, hardware or software often 382
introduce a discrete step. We have presented an example when 383
changes in the infrastructure of the satellite system introduce 384
false trends in the IWV estimates, through small discrete steps, 385
even when the user configuration is held fixed. 386

ACKNOWLEDGMENT 387

The authors would like to thank A. Niell of MIT Haystack 388
Observatory and one anonymous referee for the comments and 389
suggestions on the manuscript. The GPS data were provided by 390
the IGS. 391

REFERENCES 392

[1] J. T. Houghton, G. J. Jenkins, and J. J. Ephraums, Eds., *Climate Change: 393
The IPCC Scientific Assessment*. Cambridge, U.K.: Cambridge Univ. 394
Press, 1990. 395

[2] R. D. Cess, "Water vapor feedback in climate models," *Science*, vol. 310, 396
no. 5749, pp. 795–796, Nov. 2005. DOI: 10.1126/science.1119258. 397

[3] J. Duan, M. Bevis, P. Fang, Y. Bock, S. Chiswell, S. Businger, C. Rocken, 398
F. Solheim, T. VanHove, R. Ware, S. Mc-Clusky, T. A. Herring, and 399
R. W. King, "GPS meteorology: Direct estimation of the absolute value 400
of precipitable water," *J. Appl. Meteorol.*, no. 6, pp. 830–838, Jun. 1996. 401

[4] T. R. Emardson, G. Elgered, and J. M. Johansson, "Three months con- 402
tinuous monitoring of the atmospheric water vapor with a network of 403
Global Positioning System receivers," *J. Geophys. Res.*, vol. 103, no. D2, 404
pp. 1807–1820, 1998. 405

[5] P. Tregoning, R. Boers, D. M. O'Brien, and M. Hendy, "Accuracy of ab- 406
solute precipitable water estimates from GPS observations," *J. Geophys.* 407
Res., vol. 103, no. D22, pp. 28701–28710, Nov. 1998. 408

[6] S. I. Gutman, S. R. Sahn, S. G. Benjamin, B. E. Schwartz, K. L. Holub, 409
J. Q. Stewart, and T. L. Smith, "Rapid retrieval and assimilation of ground 410
based GPS precipitable water observations at the NOAA forecast systems 411
laboratory: Impact on weather forecasts," *J. Meteorol. Soc. Jpn.*, vol. 82, 412
no. 1B, pp. 351–360, 2004. 413

[7] T. Nilsson and G. Elgered, "Long-term trends in the atmospheric water 414
vapor content estimated from ground-based GPS data," *J. Geophys. Res.*, 415
vol. 113, no. D19, p. D19 101, Oct. 2008. DOI: 10.1029/2008JD010110. 416

[8] J. Shuanggen and O. F. Luo, "Variability and climatology of PWV 417
from global 13-year GPS observations," *IEEE Trans. Geosci. Remote* 418
Sens., vol. 47, no. 7, pp. 1918–1924, Jul. 2009. DOI: 10.1109/ 419
TGRS.2008.2010401. 420

[9] J. F. Zumberge, M. B. Heflin, D. C. Jefferson, M. M. Watkins, and 421
F. H. Webb, "Precise point positioning for the efficient and robust analysis 422
of GPS data from large networks," *J. Geophys. Res.*, vol. 102, no. B3, 423
pp. 5005–5017, Mar. 1997. 424

[10] Emardson and Derks, "On the relation between the wet delay and the inte- 425
grated precipitable water vapour in the European atmosphere," *Meteorol.* 426
Appl., vol. 7, pp. 61–68, 2000. DOI: 10.1017/S1350482700001377. 427

- 428 [11] J. Kouba, A Guide to Using International GPS Service (IGS)
 429 Products2003, Feb. [Online]. Available: [ftp://igsb.jpl.nasa.gov/igsb/
 430 resource/pubs/GuidetoUsingIGSProducts.pdf](ftp://igsb.jpl.nasa.gov/igsb/resource/pubs/GuidetoUsingIGSProducts.pdf)
 431 [12] R. Schmid, M. Rothacher, D. Thaller, and P. Steigenberger, "Absolute
 432 phase center corrections of satellite and receiver antennas," *GPS Solut.*,
 433 vol. 9, no. 4, pp. 283–293, Nov. 2005. DOI: 10.1007/s10291-005-0134-x.
 434 [13] [Online]. Available: [http://igsb.jpl.nasa.gov/igsb/station/general/
 435 igs05.atx](http://igsb.jpl.nasa.gov/igsb/station/general/igs05.atx)
 436 [14] J. M. Dow, R. E. Neilan, and G. Gendt, "The International GPS
 437 Service (IGS): Celebrating the 10th Anniversary and looking to the
 438 next decade," *Adv. Space Res.*, vol. 36, no. 3, pp. 320–326, 2005.
 439 DOI: 10.1016/j.asr.2005.05.125.
 440 [15] G. Brown and P. Y. C. Hwang, *Introduction to Random Signals and
 441 Applied Kalman Filtering*. New York: Wiley, 1992.
 442 [16] J. L. Davis, T. A. Herring, I. I. Shapiro, A. E. E. Rogers, and G. Elgered,
 443 "Geodesy by radio interferometry: Effects of atmospheric modeling
 444 errors on estimates of baseline length," *Radio Sci.*, vol. 20, no. 6,
 445 pp. 1593–1607, 1985.
 446 [17] A. E. Niell, A. J. Coster, F. S. Solheim, V. B. Mendes, P. C. Toor,
 447 R. B. Langley, and C. A. Upham, "Comparison of measurements of
 448 atmospheric wet delay by radiosonde, water vapor radiometer, GPS, and
 449 VLBI," *J. Atmos. Ocean. Technol.*, vol. 18, no. 6, pp. 830–850, Jun. 2001.



Sweden, Borås, Sweden.

Ragne Emardson received the M.Sc. degree in 458
 computer science and engineering and the Ph.D. 459
 degree in electrical engineering from the Chalmers 460
 University of Technology, Göteborg, Sweden, in 461
 1992 and 1998, respectively. 462

From 1998 to 2000, he was a Postdoctoral 463
 Researcher with the Jet Propulsion Laboratory, 464
 California Institute of Technology, Pasadena. He 465
 has also held positions with Ericsson Mobile Data 466
 Design and SAAB Ericsson Space. Since 2003, he 467
 has been with the SP Technical Research Institute of 468
 Sweden, Borås, Sweden. 469



Jan Johansson was born in Borås, Sweden, in 1960. 470
 He received the M.Sc. and Ph.D. degrees in elec- 471
 trical engineering from the Chalmers University of 472
 Technology, Göteborg, Sweden, in 1985 and 1992, 473
 respectively. 474

He is currently an Adjunct Professor with the 475
 Department of Radio and Space Science, Chalmers 476
 University of Technology, and the Deputy Head of 477
 Department at the SP Technical Research Institute of 478
 Sweden, Borås. 479

450
 451
 452
 453
 454
 455
 456
 457



Per Jarlemark was born in Hjo, Sweden, in 1962.
 He received the M.Sc. degree in engineering physics
 from Uppsala University, Uppsala, Sweden, in 1986
 and the Ph.D. degree in electrical engineering from
 the Chalmers University of Technology, Göteborg,
 Sweden, in 1997.

Since 1999, he has been with the SP Technical
 Research Institute of Sweden, Borås, Sweden.



Gunnar Elgered was born in Götene, Sweden, 480
 in 1955. He received the M.S.E.E. and Ph.D. de- 481
 grees from the Chalmers University of Technology, 482
 Göteborg, Sweden, in 1977 and 1983, respectively. 483

He is currently a Professor in electrical measure- 484
 ments, and he chairs the Department of Radio and 485
 Space Science, Chalmers University of Technology. 486
 His research is focused on remote sensing of the 487
 atmosphere using space geodetic techniques and mi- 488
 crowave radiometry. 489